Available online at www.sciencedirect.com
ScienceDirect
Bioelectrochemistry 69 (2006) 187–192
Bioelectrochemistry
www.elsevier.com/locate/bioelechem

Automatic positioning of a microinjector in mouse ES cells and rice protoplasts

Hideaki Matsuoka [a,b,*], Soichiro Shimoda [a], Yoshiyuki Miwa [c], Mikako Saito [a,b]

[a] Department of Biotechnology and Life Science, Tokyo University of Agriculture and Technology, Koganei, Tokyo 184-8588, Japan
[b] CREST (Core Research for Evolutional Science and Technology), Japan Science and Technology Agency, Honcho 4-1-8, Kawaguchi, Saitama 332-0012, Japan
[c] Faculty of Science and Engineering, Waseda University, 3-4-1 Ookubo, Shinjuku-ku, Tokyo 169-8555, Japan

Received 11 September 2005; received in revised form 15 February 2006; accepted 16 February 2006
Available online 6 March 2006

Abstract

A 2-channel (2C) microinjector was prepared by pulling a glass capillary with a θ-shaped cross section. One channel was used as a potential measuring electrode (MeaE) and the other was used as an electrophoretic introduction electrode (IntE). The 2C microinjector was propelled by an oil pressure manipulator driven by a pulse motor, while the MeaE output was recorded continuously. When the 2C microinjector penetrated the cell membrane of a mouse ES cell or a rice protoplast, the output potential changed sharply. The differential of this potential change was used as a stop signal for the pulse motor. Thus, the microinjector was correctly positioned in the cell without losing cell viability. Its success rate was 73% and 84% for ES cells and rice protoplasts, respectively. After the positioning of the microinjector in the cell, Lucifer yellow (LY) was introduced via IntE. Under these conditions, the rate of viable cells was 16% and 62% for ES cells and rice protoplasts, respectively.
© 2006 Elsevier B.V. All rights reserved.

Keywords: Microinjector; Automatic positioning; Intracellular potential; ES cell; Rice protoplast

1. Introduction

An intense need for the direct introduction of genes, expression products or associated bioactive compounds into target cells has arisen in order to analyze protein–protein interaction [1], intracellular [2,3], or intercellular [4–6], signaling, intracellular localization or trafficking [7,8], and gene targeting efficiency [9]. Thus, microinjection has now attracted substantial attention because of its potential usefulness. However, microinjection requires a high degree of expertise and is very time consuming. Therefore, it is not considered practical for the rapid treatment of large number of cells. Recently, difficulties have partially been overcome by the development of a unique machine, the single-cell manipulation supporting robot (SMSR) [10]. SMSR has enabled high-throughput microinjection. Moreover, SMSR was found to be useful for training purposes.

In spite of its usefulness, there remains a need for further improvement towards fully automatic microinjection. To accomplish this final goal, it is essential to develop a controller that can stop the microinjector at the proper position in the cell. Formerly various plates with multiple microwells or multiple pores were devised [11–18], and ideas of automatic microinjection using these plates were proposed [13,14,17]. However no successful demonstration was reported. In these cases, the microinjector was propelled to the XY-address of the center of the well or the pore. Consequently the microinjector penetrated the center of the cell and this killed most cells, except those of 50 μm or more in diameter or exceptionally resilient cells [19,20].

According to the suggestions of microinjection experts (personal communications), it is important to make the penetration depth of the microinjector as shallow as possible. Therefore, it is necessary to stop the microinjector immediately when the tip penetrates the cell membrane. However, it is difficult to determine the stop position by the XY-address based on the well or pore position, because cell diameters vary from cell to cell. Moreover, cell diameter changes due to cell deformation

* Corresponding author. Department of Biotechnology and Life Science, Tokyo University of Agriculture and Technology, Koganei, Tokyo 184-8588, Japan. Tel.: +81 42 388 7029; fax: +81 42 387 1503.
E-mail address: bio-func@cc.tuat.ac.jp (H. Matsuoka).

1567-5394/$ - see front matter © 2006 Elsevier B.V. All rights reserved.
doi:10.1016/j.bioelechem.2006.02.002

when the microinjector presses and then penetrates the cell membrane. Therefore it is necessary to use another stop signal that does not depend on these dimensional factors.

When a microelectrode is propelled towards the cell membrane at a right angle to the cell membrane, a steady potential is obtained. This potential will change sharply when the microelectrode contacts with and then penetrates the cell membrane. Subsequently, the potential again becomes steady, and this is designated as the intracellular potential. Such a potential change may be used as a stop signal that is independent of cell diameter and cell deformation.

This paper describes a novel method of automatic microinjector positioning. We have devised an electric circuit that can sensitively measure the intracellular potential without serious electric noise. Thus, the measured potential change is modified to generate an effective stop signal. The performance of the present method was then tested with mouse ES cells and rice protoplasts.

2. Materials and methods

2.1. Preparation of 2-channel microinjector

A glass capillary with a θ-shaped cross section (Fig. 1) (outer diameter, 1 mm) was heated and pulled to make the tip diameter smaller than 1 μm using a laser puller (Model 2000, Sutter Instrument Co., Novato, CA). One channel of the capillary was filled with a solution of 0.5 M KCl. Ag/AgCl wire was then inserted into the capillary to produce a potential measuring electrode (MeaE) (Fig. 1). The reference electrode for MeaE was a commercially available Ag/AgCl electrode (RE). The other channel was filled with a solution containing 0.5 M KCl and 1 mM Lucifer yellow (LY). Pt wire was inserted into the capillary to produce a dye-introducing electrode (IntE). The counter electrode (CE) for IntE was prepared by filling a glass tube with 3% agar gel containing 0.5 M KCl.

2.2. Apparatus construction

The MeaE and RE were connected to an electrometer (Fig. 1). The output of the electrometer was connected to a signal converter and a programmable controller for a pulse motor driver (SC/MD). From the output, digital pulses were generated at 25 Hz and supplied to a pulse motor connected directly to an oil pressure manipulator (OM) (MO-22, Narishige Kagaku, Tokyo). The clockwise rotation of the OM propels the microinjector. The minimum step of the microinjector is 0.25 μm and the propelling speed is 6.25 μm s^{-1}.

The IntE and CE were connected to a pulse generator (PG) via an electric isolator (Iso). Rectangular analog pulses were generated by PG, and intensified and supplied to the IntE such that the voltage of IntE was −20 V vs. CE (pulse width: 10–50 ms; pulse number: 1–5 pulses with 1 s interval). These conditions were determined so that the amount of LY expelled from the microinjector was enough for direct observation with a fluorescent microscope.

2.3. Conversion of intracellular potential signal

The output of MeaE vs. RE was amplified and input into a low-pass filter circuit. This signal was further converted to its differential and transferred to a comparator circuit. The intracellular potential or its differential was recorded on a pen recorder (Rec). Circuit parameters for the time constant and amplification factor were adjusted for mouse ES cells and rice protoplasts, respectively.

2.4. Mouse ES cells culture

Feeder free mouse ES cells were provided by H. Niwa (Center for Developmental Biology, RIKEN, Kobe) and were cultured at 37 °C in the absence of feeder cells in Glasgow

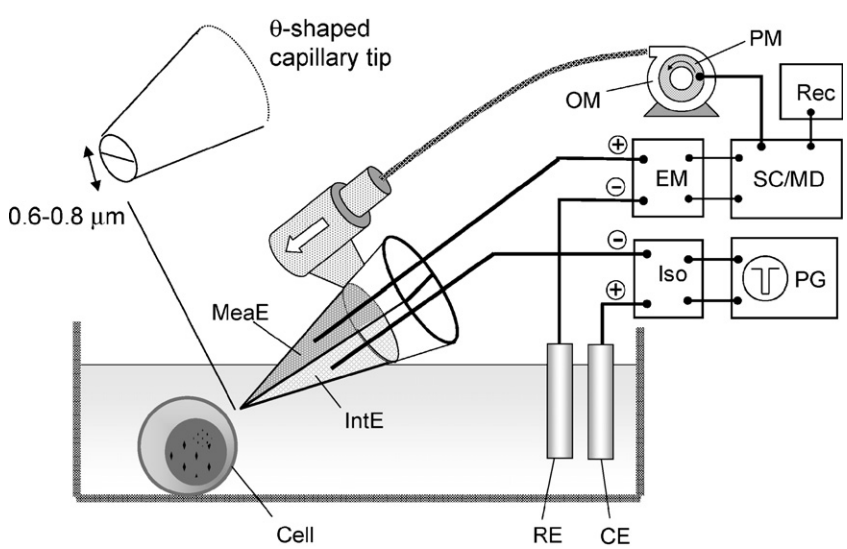

Fig. 1. Schematic diagram of an automatic microinjector positioning system. MeaE: potential measuring electrode, IntE: dye introduction electrode, RE: reference electrode for MeaE, CE: counter electrode for IntE, Iso: isolator, PG: pulse generator, EM: electrometer, SC/MD: signal converter and motor driver, PM: pulse motor, OM: oil pressure manipulator, Rec: recorder.

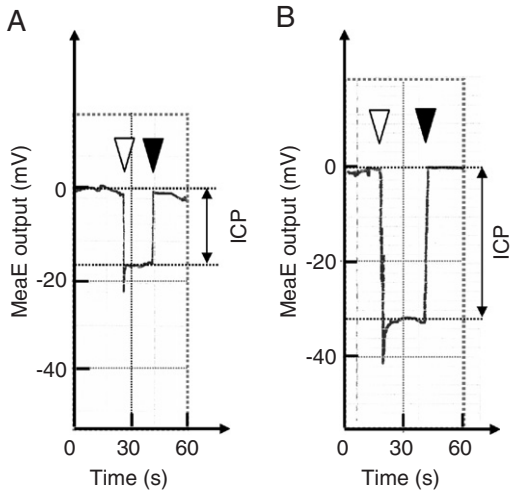

Fig. 2. Intracellular potential (ICP) of a mouse ES cell (A) and a rice protoplast (B). ▽: penetration of a microinjector into the cell, ▼: removal of the microinjector from the cell.

minimal essential medium (GMEM, Sigma, St. Louis, MO) supplemented with 10% fetal calf serum, 1 mM sodium pyruvate, 10^{-4} M 2-mercaptoethanol, 1× non-essential amino acids and 1000 U/ml of leukemia inhibitory factor (LIF) on gelatin-coated dishes (35 mm in diameter) [21]. A cell suspension containing 5000–10,000 ES cells was added to the culture dish and incubated at 37 °C.

2.5. Culture of rice cells and preparation of protoplasts

Rice cells (*Oryza sativa* L. *japonica* cv. Nipponbare) were cultured as described elsewhere [22] and 4-day-old calli were obtained. One gram of filtered calli was suspended in a 10-ml enzyme solution consisting of 0.05% (w/v) Pectolyase Y-23 (Kikkoman Corporation, Tokyo), 2% (w/v) Cellulase Onozuka RS (Yakult Honsha Co. Ltd., Tokyo), 0.01% (w/v) $CaCl_2$, 0.1% (w/v) K-dextran sulfate, and 9% (w/v) mannitol. After incubation for 1 h on a shaker (30 rpm) at 30 °C and for a further 2 h without shaking at 30 °C, the suspension was passed through a 30-μm mesh sieve to remove callus debris. The protoplasts were then collected by centrifugation (900 rpm, 2 min), washed twice with a 9% mannitol solution, and finally suspended in protoplast medium containing 9% mannitol, 1 mM $CaCl_2 \cdot 2H_2O$ and other components [23].

2.6. Evaluation of microinjection success

The success of microinjection was evaluated by microscopic observation. After the automatic positioning of the microinjector in a cell, a pulsing electric signal was applied to IntE in order to introduce LY into the cell. The LY diffusion pattern was then observed with a fluorescent microscope. Propidium iodide (PI) was added to the medium in order to confirm cell viability. Cells not stained with PI are viable because the viable cell membrane is impermeable to PI.

3. Results

3.1. Intracellular potential of mouse ES cells and rice protoplasts

A microinjector was propelled by manual operation carefully. When it penetrated the cell membrane, the output potential of the MeaE changed sharply from 0 to −16 mV (Fig. 2A). The potential seemed to change in one step, though a transient overshoot occurred. This suggests the penetration of only one membrane. When the microinjector was removed, the potential returned to the initial level. The value of −16 mV is defined as the intracellular potential and is equivalent to the cell membrane potential if the intracellular space is assumed to be homogeneous. The average (Av) and standard deviation (SD) of intracellular potential for 35 sample ES cells were −16.3 and 5.6 mV, respectively.

In the same way, the intracellular potential of rice protoplasts was measured. Plant cells have large vacuoles and therefore the microinjector must be manipulated much more carefully in order to ensure that the tip is placed in the cytosol; the narrow space between the vacuole and cell membrane. As shown in Fig. 2B, the output potential changed sharply to −33 mV with a transient overshoot. This value of −33 mV was considered to be the intracellular potential of the cytosol, although confirmation

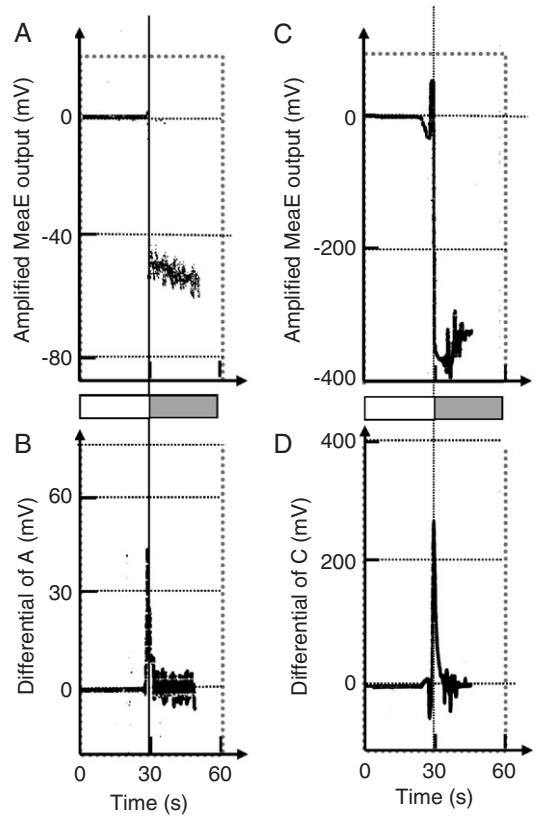

Fig. 3. Potential changes and their differentials occurring during the penetration of a microinjector through the cell membrane. (A, B): mouse ES cell, (C, D): rice protoplast, (A, C): potential changes, (B, D): differentials of potential changes. □: propelling of a microinjector, ■: holding a microinjector at the stopped position. The ordinates of B and D indicate differentiated and properly amplified values of A and C.

Table 1
Success rate of microinjector positioning and LY introduction

	Cells	(a) Number of tested cells	(b) Success of automatic positioning of microinjector	(c) Success of physical introduction of LY	(d) Number of cells unstained with PI	Success rate of total process (d)/(a)
A	Mouse ES cell	37	31	–	27	73%
	Rice protoplast	25	21	–	21	84%
B	Mouse ES cell	108	79	71	17	16%
	Rice protoplast	37	31	30	23	62%

(A) rate of viable cells after microinjector positioning alone, (B) rate of viable cells after microinjector positioning and LY introduction.

was difficult by microscopic observation alone. The Av and SD of the intracellular potential for 35 sample protoplasts were −27.8 and 16.7 mV, respectively.

A possible cause of the transient overshoot is described below under the Discussion section.

3.2. Differential of MeaE output potential

A steady intracellular potential is available but the level is variable from cell to cell. Therefore, an absolute value cannot be used as the signal of cell membrane penetration. Instead, we intended to use the differential of potential change and devised the novel apparatus depicted in Fig. 1.

A microinjector was propelled towards a mouse ES cell automatically, while the output potential of MeaE was measured continuously. When the microinjector penetrated the cell membrane, it changed sharply towards the negative (Fig. 3A). The differential is shown in Fig. 3B. When the amplitude of this differential exceeded a threshold level that was determined beforehand, a signal to stop microinjector propelling was generated. In the case of the rice protoplast, output potential (Fig. 3C) and its differential (Fig. 3D) were recorded in the same way. The differential showed a sharp pulsing signal and the microinjector could be immediately stopped.

For automatic stop control, braking distance is an important parameter. Its estimated value is described under the Discussion section. Though it was not actually measured, the present conditions caused no fatal effects in either cell.

3.3. Success rate of automatic microinjector positioning

After the microinjector was automatically stopped in the mouse ES cell, the output potential of the MeaE remained steady. This suggested successful positioning in the cell. In fact, the cell maintained its initial cell shape and appeared to maintain its viability. According to the viability criteria based on PI staining, the success rate was 73% (Table 1A). On the other hand, in the case of rice protoplasts, the success rate of automatic positioning was 84%.

3.4. Success rate of LY introduction after automatic positioning

In pressure microinjection, an amount of liquid is added to the cell and intracellular pressure is raised. On the other hand, in electrophoretic introduction, a high concentration of ionic compounds is added to the cell. Such changes in intracellular pressure or ionic conditions influence the cell viability. Therefore, the influence of LY introduction was investigated.

When the microinjector was automatically positioned in mouse ES cells, cell appearance did not change (Fig. 4B), suggesting successful positioning. LY was then introduced and its diffusion was observed. As shown in Fig. 4D, the fluorescent cell image was the same as the initial shape, thus indicating the successful physical introduction of LY. The success rate was 66% (71 out of 108 cells) (Table 1B). Cells were then stained with PI to confirm viability. In contrast to our expectations, the number of viable cells was only 17 of 71 cells (24%). This decrease in the viability rate, however, does not necessarily indicate that LY is toxic. This is speculated to be due to particular properties of ES cells as described in detail under the Discussion section.

On the other hand, in the case of rice protoplasts, the success rate of the physical introduction of LY was 81% (30/37) and the rate of viable cells after LY introduction was 77% (23/30).

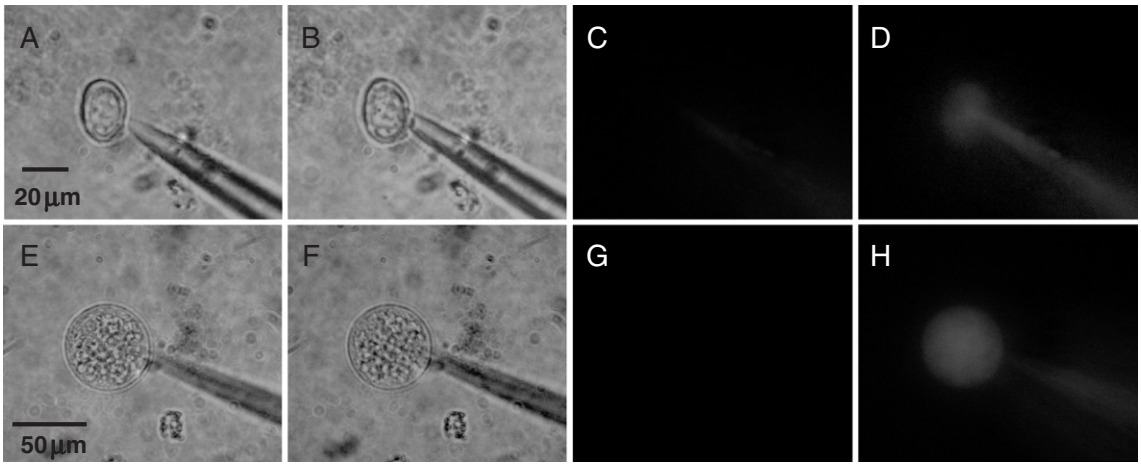

Fig. 4. Successful cases of microinjector positioning and LY introduction. (A–D): a mouse ES cell, (E–H): a rice protoplast, (A, E): before the penetration of a microinjector into the cell, (B, F): after the positioning of the microinjector rightly in the cell, (C, G): fluorescent images of B and F, (D, H): fluorescent images after LY introduction.

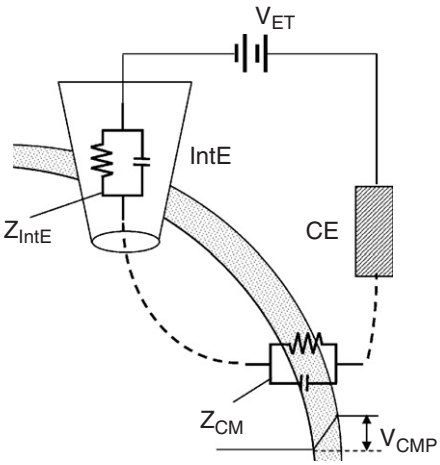

Fig. 5. Cross membrane potential speculated to be loaded.

The viability data of Table 1B is those determined at 1 h after the LY introduction. The cells which were not stained at 1 h were not stained even at 24 h. This implies that LY might not cause the cell death during successive culture.

4. Discussion

4.1. Cause of viability loss observed in ES cells

As a target cell, an ES cell is the most delicate one. In fact the microinjection into an ES cell has been extraordinarily difficult and no success has been reported until recently [10]. In this study, we applied electric voltage between IntE and CE. Since CE was placed outside of the cell, electric potential was inevitably loaded on the cell membrane (Fig. 5). The cross membrane potential (V_{CMP}) is given by $\{Z_{CM}/(Z_{IntE}+Z_{CM})\}V_{ET}$, where V_{ET} is the electric voltage applied between electrode terminals. The cell may be killed if V_{CMP} is high enough to cause unusual influx of ions and ionic molecules including LY, Cl^-, K^+, and H^+, from IntE and external medium. In the case of cultured tobacco cell line BY-2, a relation between V_{CMP} and cell viability was studied [24]. When V_{ET} was 2.0 V (inside negative) for 10 s, V_{CMP} reached 250 mV but the cell still maintained its viability. In the present study, V_{ET} is 20 V for no longer than 0.25 s (max. 50 ms × 5 times). This electric condition is not thought to be fatal to plant cells, though we have not measured actually with rice protoplasts. In fact, V_{CMP} was not crucial to rice protoplasts as shown in Table 1B. In contrast, it was fatal to mouse ES cells suggesting that they are markedly susceptible to electric or electrochemical stimulus.

4.2. Overshoot observed in the potential change occurring during the penetration

There is an overshoot in Fig. 2. This suggests a complex phenomenon occurring during the penetration. Theoretically the cell membrane potential is given by the addition of surface potential (Donnan potential), diffusion potential, and electrogenic potential. The profile just near the membrane surface (within 10–100 nm) is determined principally by the surface potential. The magnitude of the surface potential depends upon the net charge fixed on the membrane and the ionic concentration in the bulk. Since the cell membrane is suspected to have negative charge and the ionic concentration in the cell is higher than that in the external medium, a postulated profile will be given as depicted in Fig. 6.

Under this condition, when a microinjector slowly approaches and finally contacts the membrane surface, the output potential will change as shown by the arrow-a. Then the microinjector penetrates the membrane and comes in the cytosol. During this process, the potential will sharply change (arrow-b) and immediately becomes a steady level of intracellular potential level (arrow-c). The overshoot observed in Fig. 2 is speculated to be arrow-b. In this sense, the penetration may be expressed by two or more steps.

On the other hand, when the microinjector moves rapidly, the magnitude of arrow-b will apparently be reduced, or it will disappear. In fact, such an overshoot could not necessarily be observed in automatic operation mode. Anyway, such an unstable overshoot signal may not be used as a penetration signal.

4.3. Braking distance

The response profiles printed on a paper (Fig. 3) seems to be of low time resolution. But the electronic circuit has a sufficient time resolution. The differential of MeaE output was transferred to the comparator circuit. At the comparator circuit, the initial rise of the differential of MeaE was compared with a threshold potential. The threshold level was adjusted at a proper level based on many preliminary experiments. We have determined it 2.0 V for mouse ES cells. Under this condition, the delay time until the MeaE exceeded the threshold (Δt in Fig. 7) was no longer than 100 ms. The pulse motor was driven by digital pulses at 25 Hz and the microinjector was propelled 250 nm/pulse. Therefore a braking distance was estimated as no longer than 625 nm (250 × 25 × 0.1).

4.4. Dynamic behavior of LY near the microinjector tip

When electric pulses were applied to the IntE, the fluorescent intensity increased instantly around the tip of the microinjector. LY

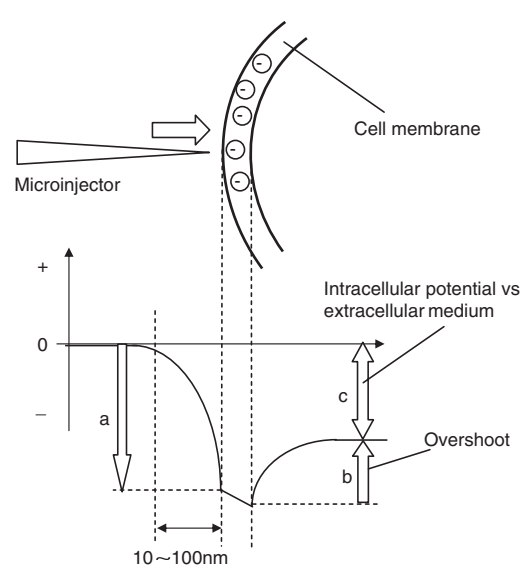

Fig. 6. Postulated profile of membrane potential.

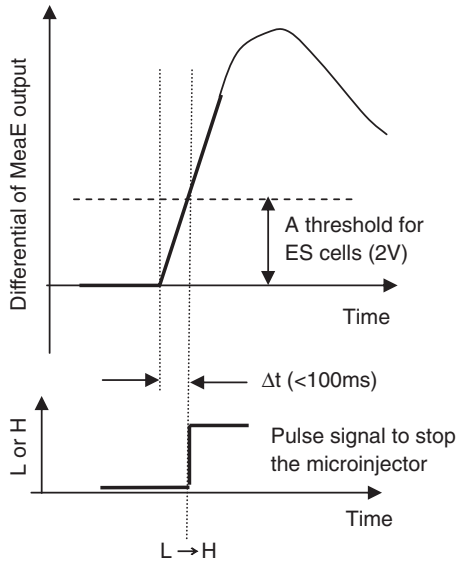

Fig. 7. Schematic diagram of the delay time until the generation of a stop signal.

seemed to rush towards the tip and the narrow passage in the microinjector seemed to be jammed with LY. In fact, the actual concentration of LY near the tip became much higher than the initial.

This is a reason the image of the microinjector in C or G of Fig. 4 was only slightly fluorescent or non-fluorescent under the present camera condition.

5. Conclusion

Microinjection difficulty depends on cell size and physical properties, such as elasticity and plasticity. ES cells are particularly difficult because of their markedly small size (10–20 μm in diameter) and sticky cell membrane. Rice protoplasts are also a difficult because of their small size (30–50 μm in diameter) and weak cell membrane. In this study, automatic positioning of the microinjector was successfully demonstrated in both types of cell. Moreover, LY introduction was also successfully performed in both cells, although marked loss of viability was observed in mouse ES cells. Further developmental studies should be focused on the increased precision with regard to introduction depth.

Acknowledgments

We thank H. Niwa and A.G. Smith for providing us with feeder free mouse ES cells. We thank Y. Nishizawa and N. Shibuya for providing us with RCC1 promoter and elicitor, respectively. This work was funded to H.M. from CREST of Japan Science and Technology Agency on the research subject: The High Throughput Creation of Disease Model Cells and the Analysis of Their Function.

References

[1] X.W. Wang, Microinjection technique used to study functional interaction between p53 and hepatitis B virus X gene in apoptosis, Mol. Biotechnol. 18 (2001) 169–177.

[2] J.H. Kim, E. Creekmore, P. Vezina, Microinjection of CART peptide 55–102 into the nucleus accumbens blocks amphetamine-induced locomotion, Neuropeptides 37 (2003) 369–373.

[3] M. Saito, Y. Mukai, T. Komazaki, K.-B. Oh, Y. Nishizawa, M. Tomiyama, N. Shibuya, H. Matsuoka, Expression of rice chitinase gene triggered by the direct injection of Ca^{2+}, J. Biotechnol. 105 (2003) 41–49.

[4] D. Giessmann, C. Theiss, W. Breipohl, K. Meller, Microinjection of actin antibodies impaired gap junctional intercellular communication in lens epithelial cells in vitro, Curr. Eye Res. 27 (2003) 157–164.

[5] D.K. Frank, B. Szymkowiak, O. Josifovska-Chopra, T. Nakashima, K.W. Kinnally, Single-cell microinjection of cytochrome c can result in gap junction-mediated apoptotic cell death of bystander cells in head and neck cancer, Head Neck 27 (2005) 794–800.

[6] M. Saito, T. Chikazawa, H. Matsuoka, Y. Nishizawa, N. Shibuya, Elicitor action via cell membrane of a cultured rice cell demonstrated by the single-cell transient assay, J. Biotechnol. 76 (2000) 227–232.

[7] Y.H. Kao, P. Sterling, Matching neural morphology to molecular expression: single cell injection following immunostaining, J. Neurocytol. 32 (2003) 245–251.

[8] S.M. Gorisch, K. Richter, M.O. Scheuermann, H. Herrmann, P. Lichter, Diffusion-limited compartmentalization of mammalian cell nuclei assessed by microinjected macromolecules, Exp. Cell Res. 289 (2003) 282–294.

[9] N.D. Tran, X. Liu, Z. Yan, D. Abbote, Q. Jiang, E.B. Kmiec, C.D. Sigmund, J.F. Engelhardt, Efficiency of chimeraplast gene targeting by direct nuclear injection using a GFP recovery assay, Molec. Ther. 7 (2003) 248–253.

[10] H. Matsuoka, T. Komazaki, Y. Mukai, M. Shibusawa, H. Akane, A. Chaki, N. Uetake, M. Saito, High throughput easy microinjection with a single-cell manipulation supporting robot, J. Biotechnol. 116 (2005) 185–194.

[11] C.C. Meek, P. Pantano, Spatial confinement of avidin domains in microwell arrays, Lab Chip 1 (2001) 158–163.

[12] M. Yang, C.W. Li, J. Yang, Cell docking and on-chip monitoring of cellular reactions with a controlled concentration gradient on a microfluidic device, Anal. Chem. 74 (2002) 3991–4001.

[13] Y. Kikuchi, Microchannel array device, method for holding particle, method for holding cell and injecting substance, and apparatus for holding cell and injecting substance, Japanese Patent, Publication Number 2002-27969.

[14] T. Takeshita, J. Otomo, S. Nomura, M. Matsunami, N. Moriya, S. Saito, Apparatus for introducing sample into amphibian oocyte, Japanese Patent, Publication Number 2002-65241.

[15] T. Yasukawa, A. Glidle, J.M. Cooper, T. Matsue, Electroanalysis of metabolic flux from single cells in picolitre-volume microsystems, Anal. Chem. 74 (2002) 5001–5008.

[16] H. Maruyama, F. Arai, T. Fukuda, T. Katsuragi, Immobilization of individual cells by local photo-polymerization on a chip, The Analyst 130 (2005) 304–310.

[17] J. Park, S.-H. Jung, Y.-H. Kim, B. Kim, S.-K. Lee, J.-O. Park, Design and fabrication of an integrated cell processor for single embryo cell manipulation, Lab Chip 5 (2005) 91–96.

[18] J.R. Rettig, A. Folch, Large-scale single-cell trapping and imaging using microwell arrays, Anal. Chem. 77 (2005) 5628–5634.

[19] B.R. Davis, J. Yannariello-Brown, N.L. Prokopishyn, Z. Luo, M.R. Smith, J. Wang, N.D. Victor-Carsrud, D.B. Brown, Glass needle-mediated microinjection of macromolecules and transgenes into primary human blood stem/progenitor cells, Blood 15 (2000) 437–444.

[20] H. Matsuoka, M. Saito, High throughput microinjection technology toward single-cell bioelectrochemistry, Electrochemistry 74 (2006) 12–18.

[21] A.G. Smith, Culture and differentiation of embryonic stem cells, J. Tissue Cult. Methods 13 (1991) 89–94.

[22] C.C. Chu, C.C. Wang, C.S. Sun, C. Hsu, K.C. Yin, C.Y. Chu, F.Y. Bi, Establishment of an efficient medium for another culture of rice through comparative experiments on the nitrogen sources, Sci. Sin. 16 (1975) 659–688.

[23] J. Kyozuka, Y. Hayashi, K. Shimamoto, High frequency plant regeneration from rice protoplasts by novel nurse culture methods, Mol. Gen. Genet. 206 (1987) 408–413.

[24] H. Matsuoka, H. Sotoyama, M. Saito, K.-B. Oh, S. Horikiri, Effects of a pulsing electric signal on the cross membrane potential and the cell division potentiality of a single cell of tobacco, Bioelectrochem. Bioenerg. 49 (1999) 65–72.